International Journal of Pharmaceutics 515 (2016) 104–113

Contents lists available at ScienceDirect

International Journal of Pharmaceutics

journal homepage: www.elsevier.com/locate/ijpharm

Half generations magnetic PAMAM dendrimers as an effective system for targeted gemcitabine delivery

Maryam Parsian[a,*], Pelin Mutlu[b], Serap Yalcin[c], Aysen Tezcaner[a,d], Ufuk Gunduz[a,e,*]

[a] Department of Biotechnology, Middle East Technical University, Ankara, Turkey
[b] Central Laboratory, Molecular Biology and Biotechnology R&D Center, Middle East Technical University, Ankara, Turkey
[c] Department of Food Engineering, Ahi Evran University, Kırşehir, Turkey
[d] Department of Engineering Sciences, Middle East Technical University, Ankara, Turkey
[e] Department of Biological Sciences, Middle East Technical University, Ankara, Turkey

ARTICLE INFO

Article history:
Received 29 June 2016
Received in revised form 5 October 2016
Accepted 6 October 2016
Available online 7 October 2016

Keywords:
Half generation PAMAM dendrimer
Gemcitabine
Magnetic nanoparticles
Chemotherapy
MCF-7
SKBR-3

ABSTRACT

Tumor-specific delivery of anticancer drugs by magnetic nanoparticles will maximize the efficacy of the drug and minimize side effects, and reduce systemic toxicity. The magnetic core of these nanoparticles provides an advantage for selective drug targeting as they can be targeted to the tumor site and accumulated in cancer cells by means of an external magnetic field. Magnetic nanoparticles can be coated with Polyamidoamine (PAMAM) dendrimer and loaded with drugs. However, biomedical applications of PAMAM dendrimers are limited due to their toxicity associated with their multiple cationic charges due to terminal $-NH_2$ groups. Modifying the positively charged end groups with negatively charged —COOH groups, is a satisfactory strategy for obtaining less toxic PAMAM dendrimers. Gemcitabine being an analogue of deoxycytidine, is an effective anticancer drug. However, clinical benefits of Gemcitabine are limited due to its short biological half-life. The aim of this study was to obtain an effective, less toxic targeted delivery system for Gemcitabine. Half generations, between G4.5 and G7.5, of PAMAM dendrimer coated magnetic nanoparticles (DcMNPs) were synthesized and conjugated with Gemcitabine. TEM images showed nanoscale size (12–14 nm) of the nanoparticles. The zeta-potential analysis indicated a decreased negativity of surface charge in drug bound dendrimer compared to the empty nanoparticles. Gemcitabine was effectively conjugated successfully onto the surface of half-generations of PAMAM DcMNPs. It was observed Gemcitabine did not effectively bind to Generations G4 and G5. The highest drug loading was obtained for DcMNPs with Generation 5.5. Empty nanoparticles showed no significant cytotoxicity on SKBR-3 and MCF-7 cells. On the other hand, Gemcitabine loaded nanoparticles were 6.0 fold more toxic on SKBR-3 and 3.0 fold more toxic on MCF-7 cells compared to free Gemcitabine. Gemcitabine loaded on Generation 5.5 DcMNPs showed a higher stability than free Gemcitabine. About 94% of the drug was retained over 6 weeks period, at pH 7.2. Due to their targetability under magnetic field, stability, size distribution, cellular uptake and toxicity characteristics the dendrimeric nanoparticles obtained in this study can be useful a delivery system for Gemcitabine in cancer therapy.

1. Introduction

Magnetic micro/nanoparticles ranging from micrometer to nanometer scale are being used in an increasing number of medical and biological applications such as magnetic resonance imaging (MRI), magnetic cell separation, enzyme and protein immobilization, hyperthermia, RNA and DNA purification, and targeted drug delivery systems (Sun et al., 2008). The magnetic nanoparticles have received great interest among cancer therapeutics due to the enormous potential stemming from their small size as well as magnetic properties (Arruebo et al., 2007). The other important properties of magnetic particles for medical applications are their low toxicity and biocompatibility (Ito et al., 2005). In addition, the controllable sizes and targeting ability to the desired site by an

* Corresponding authors at: Middle East Technical University, Department of Biotechnology, İnönü Boulevard, Universities Square, No: 1, 06800, Ankara, Turkey.
E-mail addresses: smaryamparsian@gmail.com (M. Parsian), ufukg@metu.edu.tr (U. Gunduz).

http://dx.doi.org/10.1016/j.ijpharm.2016.10.015
0378-5173/

external magnetic field are the main advantages (Gao et al., 2009; Wahajuddin, 2012).

Magnetic nanoparticles can be readily modified with various biocompatible coatings and loaded with drugs (Nune et al., 2009). The drugs, nucleic acids, and proteins can be bound either to the outer shell or inside the cavities of the polymer, such as Polyamidoamine (PAMAM) dendrimer, dextran, PEG, PLGA, PHB, and chitosan. The polymeric shells need to have active functional groups in order to bond with biomolecules (Arias et al., 2001; Khodadust et al., 2013).

In order to modify the magnetic nanoparticles, PAMAM dendrimers are excellent candidates due to good special three-dimensional structure, biocompatibility, multivalent surface, and internal cavities. PAMAM magnetic nanoparticles have both targetable and stimuli-responsive drug-delivery characteristics which can release drug at the target sites (Svenson and Tomalia, 2005; Jain et al., 2010; Taghavi Pourianazar et al., 2014). Masking the cationic charge of dendrimers and converting them into biocompatible and less toxic dendrimers by surface engineering is a rewarding strategy (Gillies and Fréchet, 2005; Pryor et al., 2014; Yang et al., 2012). PEGylation, acetylation, peptide, and carbohydrate conjugation or introducing anionic charge such as half-generation dendrimers are among the methods used to neutralize the charge of PAMAM dendrimers (Hong et al., 2004; Taghavi Pourianazar et al., 2014). PAMAM coated magnetic nanoparticles are considered to deliver Gemcitabine to the target site in a controlled manner without affecting the normal cells.

Gemcitabine (2′, 2′-diflurodeoxycytidine) is an analogue of deoxycytidine which is structurally different, by its fluorine exchange on position 2′ of furanose ring. It is a potent nucleoside analogue inhibiting DNA synthesis (Cappella et al., 2001; Alexande and Greene, 2005; Mini et al., 2006). Gemcitabine is used as anticancer drug against several solid tumors, including pancreatic, lung, ovarian, colon, bladder, and breast cancers (Martín-Banderas et al., 2013). Gemcitabine with a small molecular weight is a highly hydrophilic drug, with a short plasma half-life. Therefore, it is often administered at toxic high doses in clinical applications (Hodge et al., 2011). Furthermore, due to its hydrophilic nature, it cannot traverse cell membranes by passive diffusion and, therefore enters via nucleoside transporters that may lead to drug resistance. In addition, the use of Gemcitabine is limited by its side-effects, such as toxicity to normal cells and anemia (Liu et al., 2014; Ferrazzi and Stievano, 2014). Many approaches have been attempted to improve the *in vivo* stability and efficacy of Gemcitabine and to reduce its toxicity by loading/conjugated Gemcitabine to nanoparticle systems and to overcome drug-resistance mechanisms (Maksimenko et al., 2013). Bio-conjugation to a polymeric carrier provides an attractive strategy to deliver Gemcitabine to the tumor tissue by protecting it from degradation in plasma. In line with this approach, several lipidic conjugate (Brusa et al., 2007), squalenoyl derivatives (Couvreur et al., 2006), and PEGylated conjugates of Gemcitabine (Bekkara-Aounallah et al., 2008) have been prepared and explored for enhanced anticancer properties. However, some of these systems were limited by poor solubility, uptake by the reticuloendothelial system (RES) or lower Gemcitabine payload (Chitkara et al., 2013).

In this study, with the aim of improving bioavailability, increasing Gemcitabine payload, and other biopharmaceutical features of Gemcitabine, different half generations (G4.5, G5.5, G6.5 and G7.5) of PAMAM dendrimer-coated magnetic nanoparticles (DcMNPs) were synthesized and characterized to develop an efficient drug delivery system for cancer treatment. G5.5 DcMNP was selected as the optimum generation which can load the highest amount of the Gemcitabine.

2. Materials and method

2.1. Materials

Iron (II) chloride tetrahydrate ($FeCl_2{\cdot}4H_2O$), iron (III) chloride hexahydrate ($FeCl_3{\cdot}6H_2O$), 3-aminopropyl trimethoxysilane (APTS) [NH_2 $(CH_2)_3$-Si-$(OCH_3)_3$], ethanol, methanol, methyl acrylate, ethylene di amine, phosphate buffer saline (PBS), dimethylsulfoxide (DMSO) and Gemcitabine hydrochloride were purchased from Sigma-Aldrich (U.S.A). Trypsin-EDTA, gentamycin sulphate, trypan blue and XTT cell proliferation kit were obtained from Biological Industries, Israel Beit Haemek Ltd. (Israel). XTT cell proliferation assay was measured at UV spectrophotometer 96 well plate reader (Multiskan GO, Thermo Scientific). MCF-7 cells were provided by SAP Institute (Ankara, Turkey) and SKBR-3 was provided by Assoc. Prof. Dr. Rengul Atalay, Middle East Technical University. The cells were grown in RPMI 1640 medium supplemented with 10% heat-inactivated fetal bovine serum, 1% L-glutamine, 1% gentamicin (Biological Industries, Israel) and maintained at 37 °C in a humidified air atmosphere with 5% CO_2. Mechanical stirrer (Heidolf RZR 2021, Germany) was used in the nanoparticle synthesis. UV spectrophotometer (Multiskan GO, Thermo Scientific) was used for measuring the absorbance of the supernatants. The Transmission Electron Microscopy (FEI Tecnai G2 Spirit BioTwin), X-Ray Photoelectron spectroscopy (Rigaku Ultima-IV) and Zeta-Potential (Malvern Nano ZS90) measurements were carried in METU Central Laboratory. FT-IR analysis was carried out at Associate Prof. Dr. Bora Mavis's laboratory in Hacettepe University, Mechanical Engineering Department.

2.2. Preparation and surface coating of MNPs

Bare magnetic nanoparticles were synthesized by co-precipitation methods and were coated by APTS as described by Gupta & Gupta (Gupta and Gupta, 2005). Surface coating of MNPs by PAMAM dendrimer was achieved by divergent method. A two-step series synthesis should be repeated to obtain a PAMAM dendrimer. The first step involves the addition of methylacrylate methanol solution (20%, v/v) to G0 DcMNPs, and mixing at room temperature for 7 h by ultrasonic water bath or mechanical stirrer (Gao et al., 2005; Khodadust et al., 2013; Taghavi Pourianazar et al., 2014). The first step produces a half generation.

The half generation DcMNPs obtained were separated by magnetic decantation and washed with methanol. In the second step ethylenediamine-methanol solution (50%, v/v) was added and the suspension was mixed for additional 3 h for completing the full generation. The stepwise growth of dendrimers was repeated until the desired number of generations was achieved (Yang et al., 2012; Khodadust et al., 2013). For achieving anionic carboxyl end groups, the synthesis was ended after methylacrylate addition at the desired half generation (Fig. 1).

2.3. Gemcitabine loading on different half-generations of DcMNPs

During the incubation period there was no energy input to the reaction so the conjugation of drug to the nanoparticles was supposed to occur as result of an electrostatic interaction rather than covalent bonding. Various amounts of Gemcitabine in methanol solution were incubated with G4.5, G5.5, G6.5, and G7.5 DcMNPs (2.5 mg/ml) for 24 h at room temperature. After the incubation period, Gemcitabine-conjugated DcMNPs were separated by magnetic field and conjugation efficiency was quantified by measuring the absorbance of the supernatant at 269 nm by a UV spectrophotometer. The percentage of Gemcitabine conjugated was calculated with the help of a standard curve with known concentration of Gemcitabine (Eq. (1)) and converted to μM

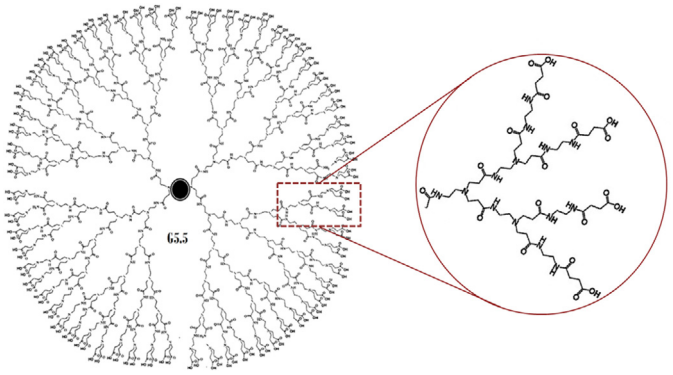

Fig. 1. Generation 5.5 PAMAM dendrimer magnetic nanoparticle with carboxyl end group.

(Parsian et al., 2016). The conjugation of Gemcitabine to DcMNPs was confirmed by FTIR, XPS and Z-potential analyses.

$$\text{Loading efficiency}(\%) = \frac{\text{Calculated drug concentration}}{\text{Theoretical drug concentration}} \times 100 \quad (1)$$

2.4. Release of Gemcitabine from DcMNPs

The release of Gemcitabine from DcMNPs was studied in acetate buffers at pH 4.2 and 5.2 for 24 h. The amount of released Gemcitabine was determined by measuring the absorbance of the release media at 269 nm using the standard curve constructed with known concentrations of Gemcitabine.

2.5. Stability of Gemcitabine conjugated on DcMNPs

The stability of DcMNPs loaded with the highest amounts of Gemcitabine was studied in PBS (pH 7.2) up to 6 weeks at 37 °C. The amount of Gemcitabine released from nanoparticles in PBS buffer was determined at defined incubation periods by measuring the absorbance of PBS buffer at 269 nm.

2.6. Magnetic field induction

In order to examine the magnetic properties of the particles, a specific slide with 3 wells connected by a canal was designed by Assist. Prof. Dr. Ender YILDIRIM (Cankaya University Department of Mechanical Engineering). MCF-7 (2×10^4 cells/slide) cells were seeded to the slide and incubated for 12 h. The medium was then removed and DcMNPs dispersed in medium was injected to the canal. The magnetic field was just applied under the middle well of the slide. The slide was incubated 4 h with magnetic field in the incubator. After incubation period the medium with DcMNPs were removed and washed with phosphate buffered saline (PBS) for complete removal of DcMNPs from cells. MCF-7 cells inside the middle well of the slide were visualized by the light microscope.

2.7. Cellular uptake of DcMNPs

DcMNPs were diluted in medium containing 10% FBS at the 2.5 mg/ml concentration and incubated for 5 h at 37 °C. After the incubation, media with DcMNPs were removed and cells were washed with PBS for complete removal of DcMNPs. Fresh media were then added to continue further viability and internalization studies. Cellular uptake of DcMNPs was detected by Prussian blue staining method (Taghavi Pourianazar and Gunduz, 2016). Nanoparticle treated and untreated MCF-7 cells were visualized under the microscopy (Fluorescence Microscope System DM6000, Leica).

2.8. Cell proliferation assay

Cytotoxicity of bare and Gemcitabine conjugated DcMNPs was determined using XTT cell proliferation assay kit. SKBR and MCF-7 (6×10^3cells/well) cells were seeded to 96 well plates and incubated in a carbon dioxide incubator at 37 °C. The viability of cells that were exposed to free DcMNPs, free Gemcitabine and Gemcitabine conjugated DcMNPs for 72 h at 37 °C was determined using XTT assay according to the manufacturer's instructions. From the cell viabilities IC_{50} values were determined. The viability of the untreated control cells was taken as 100%.

3. Results

3.1. Gemcitabine loading efficiency of DcMNPs

Dendrimer coated MNPs (G4–G7) were fully characterized and reported by our group previously. These dendrimeric nanoparticles were shown to have superparamagnetic properties by Vibrating sample magnetometer analyses (VSM) at 25 and 37 °C. The average diameter of the bare MNPs was found as 55 ± 15 nm by Dynamic light scattering analysis (DLS) (Khodadust et al., 2013).

In our initial attempts, loading of Gemcitabine on full generation PAMAM dendrimers (G4 and G7) could not be achieved. This was probably due to the amine end groups, which might have prevented the conjugation of cationic Gemcitabine. Changing the solvents such as methanol, PBS, and water didn't improve the loading of the drug. Then, half-generations of PAMAM dendrimers (G4.5–G7.5) with free carboxyl groups were synthesized, characterized and successfully loaded with Gemcitabine.

Conjugation efficiencies of different half generations (G4.5, G5.5, G6.5, and G7.5) of DcMNPs were determined at different drug concentrations (25, 50, 75 μM/ml in methanol). The highest conjugation efficiency among half generations was observed for G5.5 DcMNPs (Fig. 2). The drug conjugation efficiencies of G5.5 DcMNPs were found as 14, 20 and 24 μM for initial drug concentrations (25, 50, 75 μM/ml) of Gemcitabine, respectively. The highest drug conjugation was found as 24 μM (32%) Gemcitabine (Fig. 2), for G5.5 DcMNPs at 75 μM/ml initial drug concentration.

3.2. Characterization of PAMAM magnetic nanoparticles (DcMNPs)

Full (G5) and half generations (G4.5, G5.5, G6.5, G7.5) of DcMNPs, and Gemcitabine conjugated DcMNPs were characterized by TEM, zeta potential, FTIR and XPS analyses. The highest drug

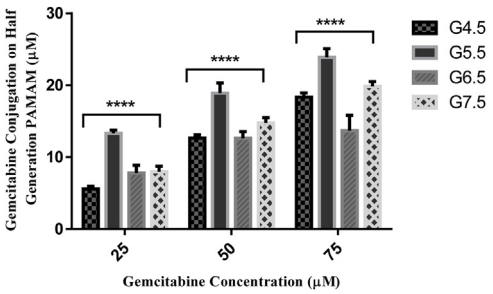

Fig. 2. Conjugation efficiencies of Gemcitabine for different half-generations DcMNPs (2.5 mg/ml). The data are represented as the mean ± SEM (n = 5), stars show statistical difference between G5.5 and G4.5, G6.5 and G7.5 at different concentrations of Gemcitabine (**** for $p < 0.0001$).

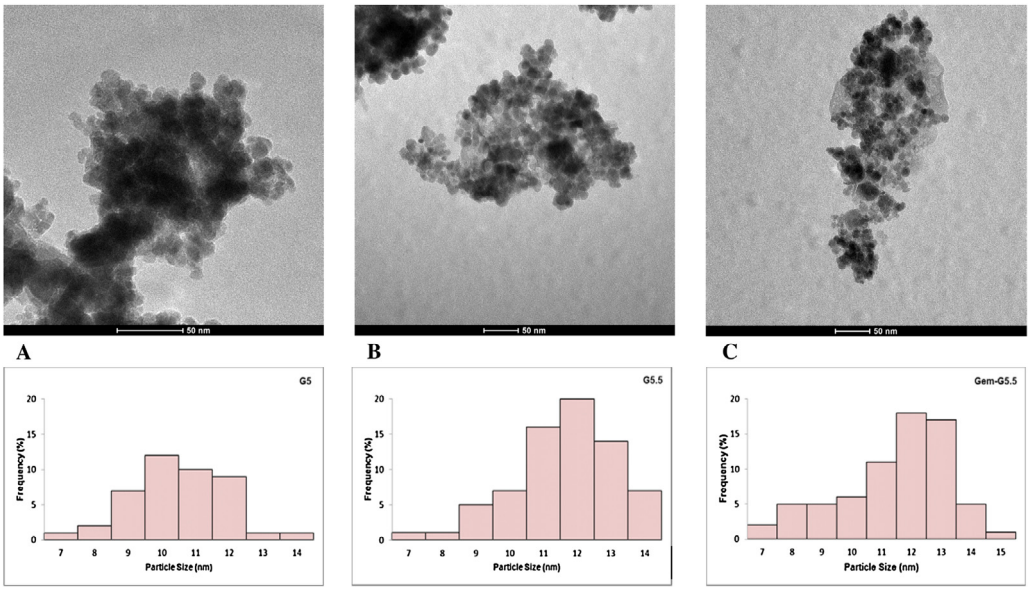

Fig. 3. TEM images and size distribution histograms of G5DcMNPs (A) G5.5 DcMNPs (B) and Gemcitabine conjugated G5.5 DcMNPs (C).

conjugation concentration was found for G5.5 DcMNPs (24 μM) and this generation of DcMNPs was used for all experiments.

3.3. TEM analysis

TEM images of G5DcMNPs and G5.5 DcMNPs are shown in Fig. 3(A and B). There were no significant differences between the full and half generations of dendrimeric nanoparticles in terms of sizes and shapes. The average diameters of G5DcMNPs and G5.5 DcMNPs were around 10–12 nm and 11–13 nm, respectively. TEM images of Gemcitabine conjugated G5.5DcMNPs (Fig. 3C) showed almost spherical morphology and uniform size distribution. The particle size of DcMNPs did not change after conjugation with Gemcitabine.

3.4. Zeta (ζ) potential analysis

The zeta potential values of DcMNPs were measured at pH 7.2. Full generation DcMNPs were positively charged with a surface potential greater than +19 mV due to the presence of protonated amine groups of dendrimer on the surface of particles. On the other hand, G5.5 DcMNPs had negative zeta potential (−10 mV) due to the presence of terminal carboxyl groups in aqueous solution. The zeta potential of Gemcitabine conjugated G5.5 DcMNPs was also negative (−4.85 mV). These results supported our hypothesis that Gemcitabine conjugation was achieved on the surface of the nanoparticles with negatively charged carboxylic groups.

3.5. Fourier transform-infrared spectroscopy (FT-IR)

Coating of DcMNPs with a PAMAM dendrimer layer of G5 and G5.5 was validated by FT-IR. Significant difference was observed at 1650–1750 cm^{-1} and 2800–3000 cm^{-1} in the FTIR spectra of G5DcMNPs and G5.5DcMNPs (Fig. 4). The COOH bonds on G5.5 DcMNP can be seen at 1730 cm^{-1}. Vibration of CO—NH— bonds for G5 DcMNP was observed at 1450, 1490, 1530, and 1620 cm^{-1}. The bands after 3000 cm^{-1} that mostly belong to N—H bonds were not observed as expected for G5.5 DcMNPs. FTIR spectra of Gemcitabine revealed high intensity broad bands at approximately 2932 cm^{-1} (CH2), 1689–1835 cm^{-1} (C=O), and 1616 cm^{-1} (NH_2) (Yalcin et al., 2014). These peaks were observed in the spectrum of Gemcitabine loaded DcMNPs. When the FTIR spectra of G5.5 and Gem-G5.5 DcMNPs were compared a difference in the peaks between 1680–1800 cm^{-1} and 2800–3200 cm^{-1} was observed.

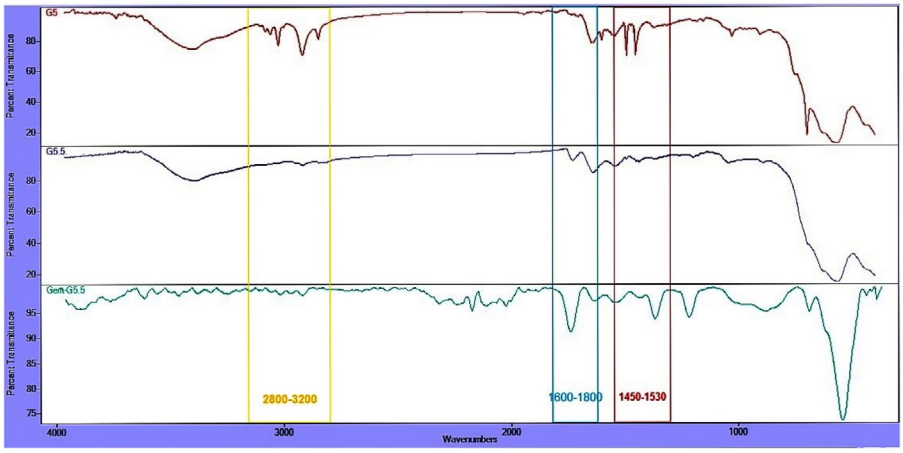

Fig. 4. FT-IR spectra of the G5 DcMNPs, G5.5 DcMNPs, and Gemcitabine conjugated G5.5 DcMNPs.

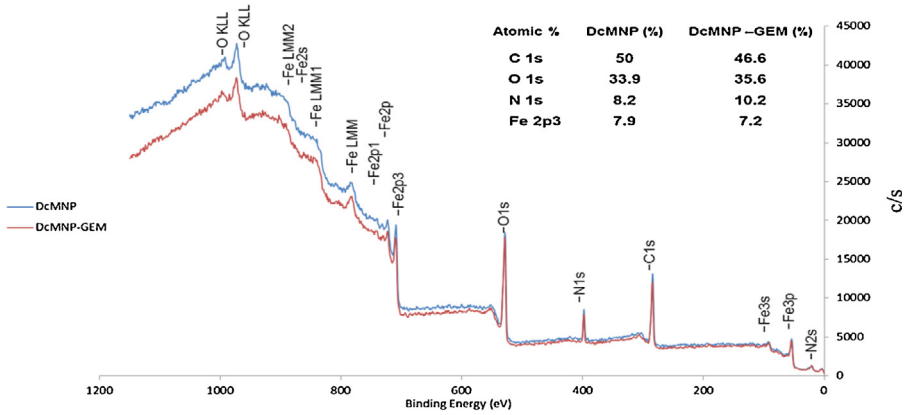

Fig. 5. XPS scanning spectra of G5.5 DcMNPs, and Gemcitabine conjugated G5.5 DcMNPs.

These peaks belong to CO—NH bonds. The peak at 3200–3400 cm^{-1} shows stretching vibration of OH, and the band at 3320 cm^{-1} was assigned to stretching vibration of NH group.

3.6. X-ray photoelectron (XPS) analyses

XPS was used to examine the shell structure of the synthesized product because core electron lines of ferrous and ferric ions can both be detectable and distinguishable in XPS. Fig. 5 shows representative XPS spectra of the G5.5 DcMNPs and Gemcitabine conjugated G5.5 DcMNPs. The N1s band of DcMNPs at 400 eV was assigned to amino groups (—NH_2). There was an increase in the contents of oxygen (O1s) from 33.9% to 35.6%, and nitrogen (N1s) from 8.2% to 10.2% in Gemcitabine conjugated DcMNPs (Fig. 5). The specific spectrum analysis of Gemcitabine conjugated DcMNPs showed the fluorine atom found in the structure of Gemcitabine. It was observed in XPS between 650 and 700 eV binding energy and under 4000 c/s (not seen in this Fig. 5). These results demonstrated that Gemcitabine was conjugated successfully to G5.5 PAMAM dendrimeric magnetic nanoparticles.

3.7. Release profiles of Gemcitabine from G5.5 PAMAM DcMNPs

Gemcitabine release studies were performed in acetate buffer at pH 4.2 and 5.2 for 24 h and the amount of released drug was determined spectrophotometrically using the calibration curves constructed with known concentrations of Gemcitabine in acetate buffer prepared at the given pH (Fig. 6). At pH 4.2, the drug was released entirely, while at pH 5.2 nearly 75% of the drug was released within the first 15 h.

3.8. Stability of Gemcitabine conjugated G5.5 PAMAM DcMNPs

The stability of Gemcitabine loaded nanoparticles was evaluated up to 6 weeks in PBS (pH 7.2) at 37 °C, which mimics the physiological conditions in blood stream (Fig. 7). Only 6% drug release occurred from Gemcitabine loaded nanoparticles during 6 weeks, which would provide an advantage in drug delivery applications.

3.9. Targetability characteristics of DcMNPs by magnetic field

In order to examine the targetability of nanoparticles, the cells were cultured in the wells of a specifically designed slide and incubated for 12 h. A magnet was placed under the middle well of the slide to study the magnetic property of the particles. DcMNPs were shifted to the middle well right away and accumulated as seen in the light microscope image. When the slide was removed away from the magnetic field, DcMNPs have dispersed in the medium again (Fig. 8).

3.10. Cellular uptake of DcMNPs

The next step was done to demonstrate the uptake magnetic nanoparticles by cancer cells. G5.5 DcMNPs, dispersed in the medium were internalized by the cells (Fig. 9). The blue colored DsMNPs are those that were taken up by the cells during 5 h of incubation and the color of the cells appeared darker than the control cells. The color of nuclear membrane appeared significantly became darker than in the control cells. This implies the accumulation of DcMNPs around the nucleus during the incubation period. The agglomerates formed after the staining of DcMNPs

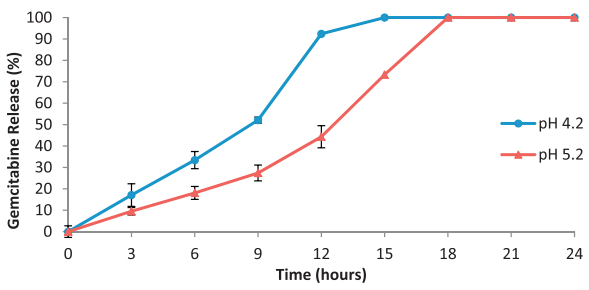

Fig. 6. Gemcitabine release profiles of DcMNPs in acetate buffer at pH 4.2 and 5.2. The data are represented as the mean ± SEM (n = 3).

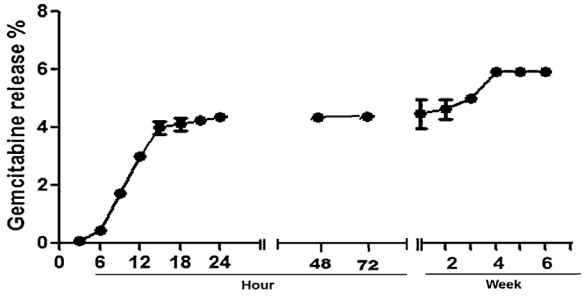

Fig. 7. Stability of Gemcitabine conjugated G5.5 DcMNPs in PBS buffer (pH 7.2). The data are represented as the mean ± SEM (n = 3).

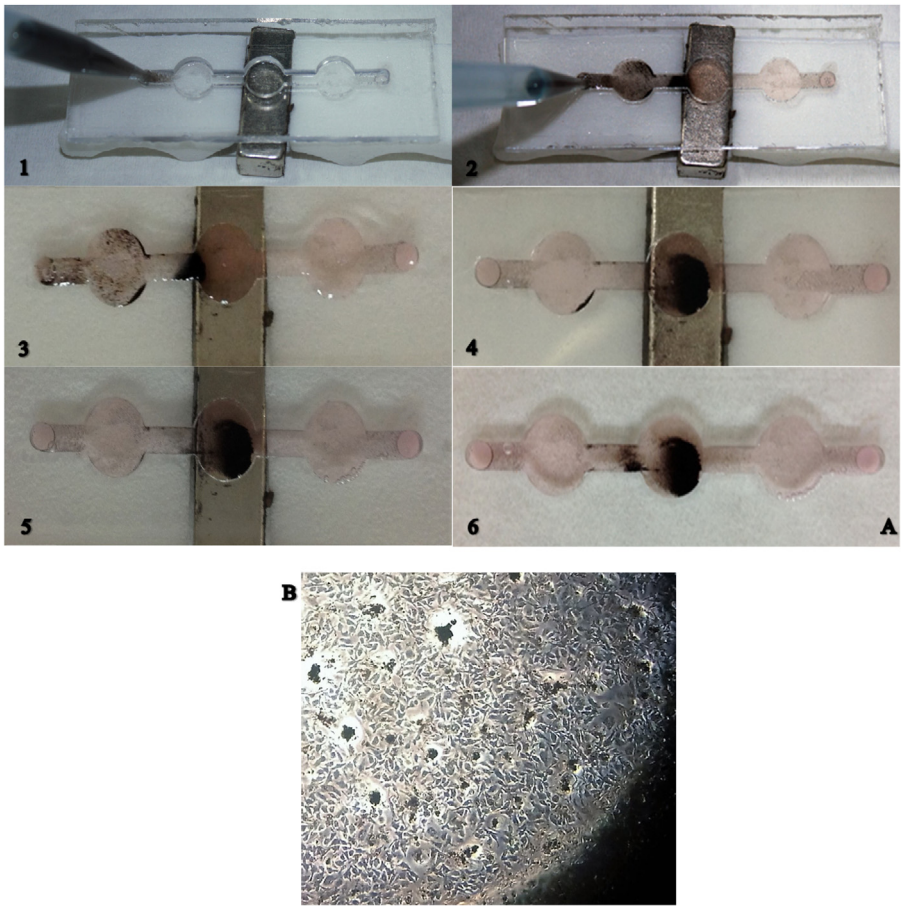

Fig. 8. Targetability characteristics of DcMNPs by the magnetic field. A: step by step application of DcMNPs to the MCF-7 cells seeded in slide. B: light microscopy image of MCF-7 cells and accumulation of MNPs in the middle well of the slide.

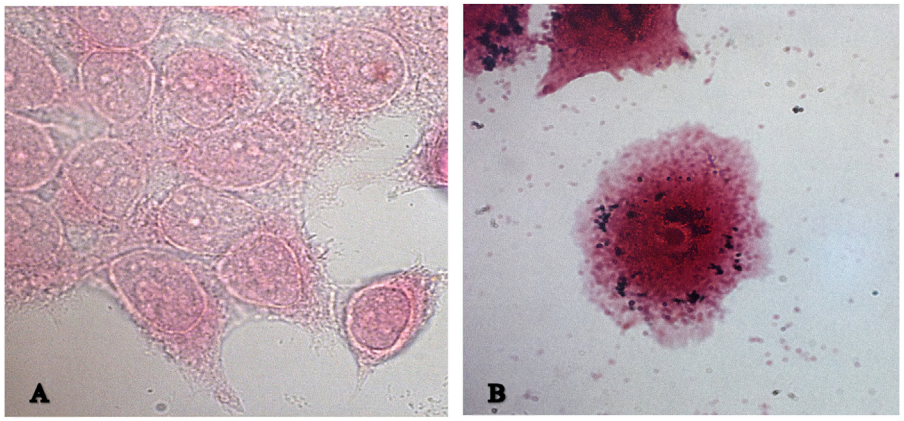

Fig. 9. The bright field microscope images of (A) untreated control MCF-7 cells, and (B) Prussian Blue stained G5.5 DcMNPs treated MCF-7 cells. The blue color indicates DcMNPs and the pink color indicates MCF-7 cells. (For interpretation of the references to colour in this figure legend, the reader is referred to the web version of this article.)

were observed as adhered on the cells even after the harsh washing of MCF-7 cells.

3.11. In vitro *cytotoxicity studies of G5.5 PAMAM DcMNPs*

Cytotoxicities of G5.5 DcMNPs, free Gemcitabine and Gemcitabine conjugated G5.5 DcMNPs were investigated by XTT cell proliferation assay using SKBR-3 and MCF-7 breast cancer cell lines. Survival rates of cells incubated with G5.5 DcMNPs indicated that there was no significant cytotoxic effect of the free nanoparticles (not loaded with Gemcitabine) on SKBR-3 and MCF-7 cells up to 1.67 mg/ml and 0.83 mg/ml concentrations, respectively (Fig. 10).

Fig. 11 demonstrates the dose dependent anti-proliferative effect of Gemcitabine loaded G5.5 DcMNPs on SKBR-3 and MCF-7 cell lines. In MCF-7 cells, IC_{50} values of Gemcitabine and Gemcitabine conjugated nanoparticles were found as 3.9 μM and 1.1 μM, respectively. IC_{50} values of Gemcitabine and Gemcitabine conjugated nanoparticles were found to be about 6.5 μM and 1.2 μM for SKBR-3 cells, respectively. Results showed that

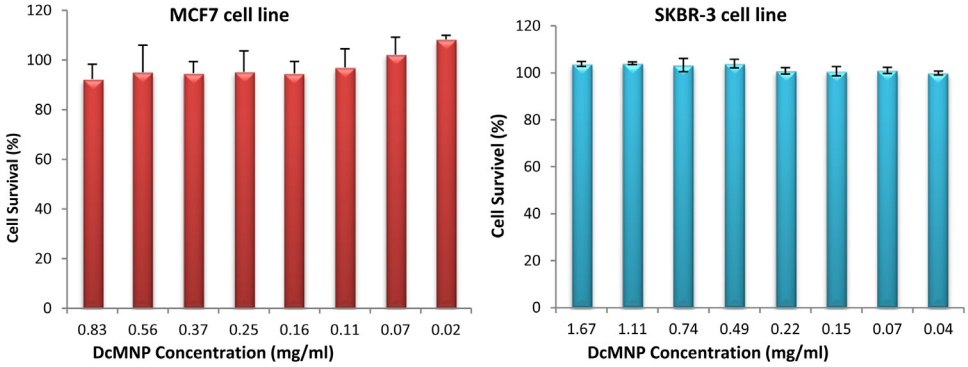

Fig. 10. Dose dependent cytotoxicity of G5.5 DcMNPs on MCF-7 and SKBR-3 cell lines. The data are represented as the mean ± SEM (n = 3).

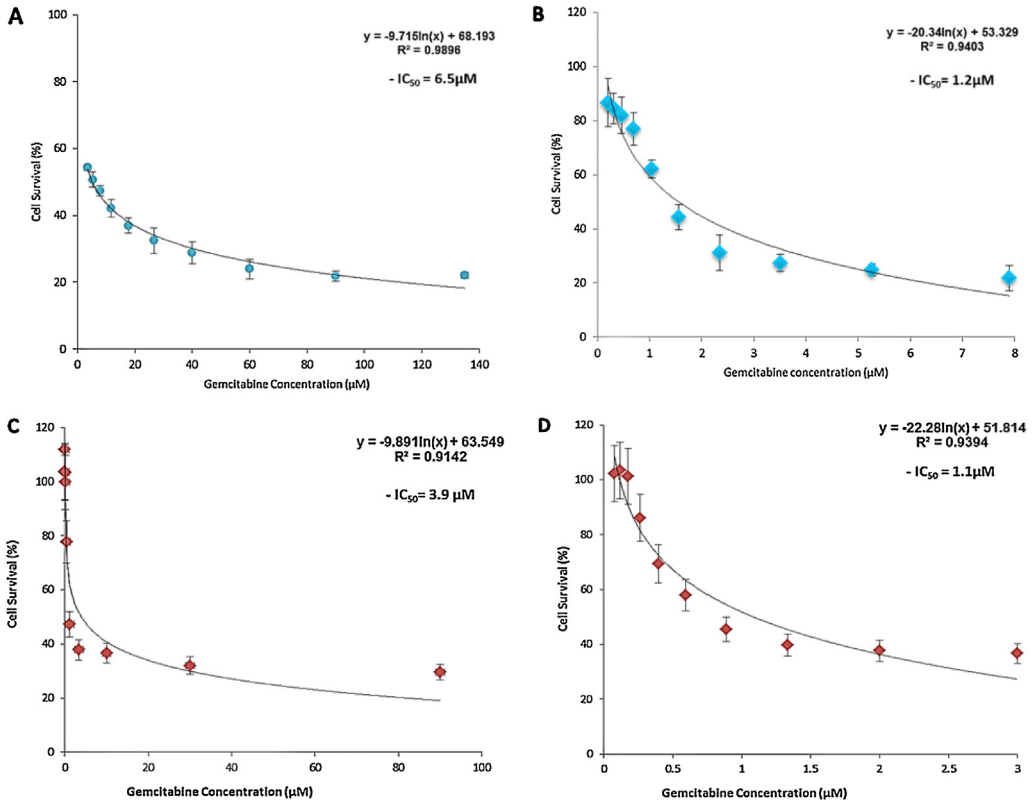

Fig. 11. IC_{50} values of (A) Gemcitabine, (B) Gemcitabine conjugated DcMNPs on SKBR-3 cells and (C) Gemcitabine, (D) Gemcitabine conjugated DcMNPs on MCF-7 cells determined using XTT cell proliferation assay. The data are represented the mean ± SEM (n = 3).

Gemcitabine loaded DcMNPs were nearly 3.6 and 5.5 fold more toxic compared to free Gemcitabine on MCF-7 and SKBR-3 cells, respectively. These results showed that Gemcitabine loaded on DcMNPs were more effective on both breast cancer cell lines.

4. Discussion

Current chemotherapeutic regimens suffer from nonspecific toxicities and drug resistance problems which limit their therapeutic potential. An alternative to overcome these limitations is developing multifunctional nanoparticles, on which the anticancer drugs could be attached. These nanoparticles could target the tumor cells either by decorating the surface of the nanocarriers with different targeting ligands or using a magnetic core. Some specific molecules are added to the nanocarrier systems to target the receptors and proteins on cancer cells. In a study, it was shown that HER2-Gem-Chitosan-nanoparticles displayed higher cytotoxicity in PANC-1 and MiaPaca-2 cells as compared to free Gemcitabine (Arya et al., 2011). Another targeted formulation which is composed of arginine-glycine-aspartic acid conjugated Bovine Serum Albumin (BSA) NPs with Gemcitabine showed higher cytotoxicity and significantly higher cellular uptake in BxPC-3 cells as compared to free Gemcitabine (Ji et al., 2012). In targeted delivery of Gemcitabine, EGFR-specific monoclonal antibody conjugated to the surface of PLGA-polyethylene glycol NPs resulted in significantly greater cytotoxicity in MiaPaCa-2 cells (Aggarwal et al., 2013).

The targeted drug delivery system possessing a magnetic core has received specific attention due to the simplicity, ease of synthesis, and ability to tailor the properties for specific purposes. These nanoparticles carrying the anticancer agent can be targeted to the tumor site, and accumulated in cancer cells by the help of an implanted permanent magnet or an externally applied field (Gao et al., 2009). Previously, magnetic nanoparticles covered with

various polymers were designed. Viota et al. developed composite nanoparticles consisting of a core of magnetite nanoparticles, coated with successive layers of high molecular weight poly (acrylic acid) and chitosan, and a final layer of folic acid. It was designed as a drug vehicle capable of delivering the anti-tumor drug Gemcitabine (Viota et al., 2013).

In another study, Mu et al. designed a small and stable nanocarrier to increase Gemcitabine's circulation time and overcome the blood–brain barrier for glioblastoma multiform therapy. The nanocarrier is made of iron oxide-based NPs immobilized with Gemcitabine, chlorotoxin, and hyaluronic acid. The nanoparticles were loaded with Gemcitabine and then, glioblastoma targeting peptide, chlorotoxin, was attached. The results indicated the potential of the nanoparticles to improve the *in vivo* performance of Gemcitabine (Mu et al., 2016).

In the previous studies of our laboratory, the synthesis and characterization of PAMAM coated magnetic nanoparticles (DcMNPs) were described as drug delivery vehicles (Khodadust et al., 2013). These DcMNPs contain internal magnetic cores and exterior polyamidoamine polymer with cationic amine end groups. Electrostatic interaction can occur between the PAMAM dendrimeric end groups of the nanoparticles and the drugs (Garg et al., 2011). Hydrolysable and biodegradable bonding of drug and surface groups of the dendrimers provide the opportunity for drug release control (Jain et al., 2010; Garg et al., 2011; Pan, 2005). However, these amine terminated nanoparticles have some disadvantages. One of the most prevalent drawbacks of cationic PAMAM dendrimers is their cytotoxicity due to the interaction with cellular membranes which can result in cell lysis (Pryor et al., 2014; Svenson, 2009). This can be overcome by modifying the dendrimer end groups with anionic or neutral moieties. Functionalization of PAMAM dendrimers with polyethylene glycol (PEG) increases the circulation time of the nanoparticle by lowering its hepatic capture and cytotoxicity (El-Sayed et al., 2002; Bildstein et al., 2011).

In this study, binding of Gemcitabine to full generations (G4 and G7) of PAMAM dendrimeric nanoparticles could not be achieved. This could probably due to the amine end group of full generation, which prevented the conjugation of Gemcitabine. Then, we synthesized and characterized the half-generations of PAMAM DcMNPs (G4.5 up to G7.5) with anionic carboxyl end groups which came out to be much better Gemcitabine carriers.

Previously, Khodadust et al. (2013) reported bare G4DcMNPs as severely cytotoxic at concentrations of higher than 250 μg/ml (Khodadust et al., 2013). Our results demonstrated that the empty half generation PAMAM dendrimeric nanoparticles have no cytotoxicity on SKBR-3 and MCF-7 cell lines over 250 μg/ml concentration. Survival rates of G5.5 DcMNPs indicated that there was no significant cytotoxic effect of the nanoparticles on SKBR-3 and MCF-7 cells up to 1.67 mg/ml and 0.83 mg/ml concentrations, respectively. Another disadvantage showed by different studies is that the cationic nanoparticles can activate platelets and induce platelet aggregation. However, nanoparticles can be engineered to prevent platelet aggregation (Cejas et al., 2007). Dobrovolskaia et al. used several formulations of PAMAM dendrimers, varying in size and surface charge, and studied their effects on human platelets *in vitro*. Their results showed that the cationic amine-terminated PAMAM dendrimers (G4–G6) induce platelet aggregation *in vitro*. However, no aggregation was detected in platelet rich plasma treated with the small cationic PAMAM (G3) and also the anionic (carboxy-terminated) and neutral (hydroxy-terminated) PAMAM dendrimers irrespective of particle size and generation (Dobrovolskaia et al., 2012). Furthermore, the reported results by Greish et al. showed coagulation toxicity *in vivo* in mice treated with cationic but not anionic PAMAM dendrimers (Greish et al., 2012). These results demonstrated that both surface charge and particle size are important physicochemical properties which determine the interaction of dendrimers with human platelets (Dobrovolskaia et al., 2012; Greish et al., 2012).

TEM images showed no size difference between full and half-generation PAMAM DcMNPs before and after drug conjugation. The Zeta-potential results of G5.5 DcMNPs demonstrated the negative charge of carboxyl terminated half generation dendrimers and nearly neutral charge after conjugation by Gemcitabine. In our study, changing the surface of the nanoparticles to the anionic PAMAM dendrimers eliminated both disadvantages of the cationic dendrimers. In other words, the anionic charged half generation DcMNPs and neutral charged Gemcitabine conjugated G5.5 DcMNPs obtained in this study are not expected to cause lysis of red blood cells and platelet aggregation (Dobrovolskaia et al., 2012; Greish et al., 2012).

The best conjugation efficiency of Gemcitabine through conjugation was obtained for G5.5 PAMAM dendrimers. The optimum loading concentration was determined as 24 μM. It is important to emphasize that we used a much lower dose (24 μM) of Gemcitabine compared to other *in vitro* studies. In a study performed by Khare et al., monomethoxy polyethylene glycol amine-polylactide-co-glycolide (mPEG-PLGA) co-polymer was utilized for passive targeting of Gemcitabine to tumor tissue. Gemcitabine loaded mPEG-PLGA nanoparticles indicated drug loading as 7.07 ± 0.35 μg (Khare et al., 2016). The nanoparticles are distributed homogeneously around a size of 200 nm (Khare et al., 2016).

The drug resistance and short plasma half-life in humans and mice (approximately 30 min) are the main obstacles for clinical use of Gemcitabine (Chitkara et al., 2013; Bildstein et al., 2010; Mu et al., 2016). Loading the Gemcitabine onto nanoparticles may help to prevent these problems.

Gemcitabine is frequently associated with multidrug resistance (MDR) phenotype. Resistance to chemotherapy has been generally correlated to the presence of molecular pumps, in tumor cell membranes that actively pump out drugs from cells (Chang, 2003; Choi and Yu, 2013). Due to hydrophilicity, Gemcitabine could not cross the plasma membrane passively. Therefore, it must be transported into the cells by nucleoside transporters (NTs), such as the human Equilibrative Nucleoside Transporters (hENT) or human sodium gradient coupled nucleoside transporters (Mini et al., 2006; Martín-Banderas et al., 2013; Hodge et al., 2011). It has been reported that Gemcitabine resistance is related to the reduced level of the hENT1 transporter (Alexander and Greene, 2005). Clinical data demonstrated that patients with tumors along with a lowered expression of hENT1 have a considerably lower survival rate following Gemcitabine therapy compared to patients with tumors that have a higher level of hENT1 (Bildstein et al., 2010; Lansakara et al., 2012). Nanoparticles loaded with cancer drugs can efficiently intrude into the tumor cells by endocytosis, forming endosomes (Lunov et al., 2010; Park et al., 2010). This route of internalization bypasses the transporters, and the drug resistance can be prevented.

In a study performed by Zhang et al., the cellular uptake of PAMAM-NH2 dendrimers by resistant breast cells were analyzed. They detected the fluorescent intensity of FITC-labeled PAMAM in MCF-7 and MCF-7-resistant cells, which included the fluorescence from the cytoplasm and endosomes/lysosomes in each cell. It is reported that the nonspecific binding was due to ionic interaction and PAMAM dendrimers can bind with proteoglycans on the cell membranes (Zhang et al., 2016). Our findings are also consistent with these results emphasizing the electrostatic interactions as the internalization route of PAMAM nanoparticles to the cells. The negative domains of the cell membrane can interact with Gemcitabine loaded DcMNPs by nonspecific electrostatic interactions to facilitate their cellular uptake. In addition to surface

charge, it was found that the cellular uptake was heavily dependent on size (Kulkarni and Feng 2013). In this study, it is shown that DcMNPs were successfully taken up by MCF-7 cells.

The control of drug release in the cells can be achieved according to variations in pH. pH responsive drug carrier systems can release the drug more efficiently in lower pH values. Tumor tissue has an extracellular pH between 6.5 and 7.2, endosomes and lysosomes have pH values between 4.5 and 6. Therefore pH responsive drug carrier systems can either target the extracellular tumor tissue or intracellular compartments (Pourjavadi and Tehrani 2016). In this study, Gemcitabine release from DcMNPs showed pH dependent release pattern. It was observed that Gemcitabine release was higher at pH 4.2 than pH 5.2. As the pH was lowered, the drug release increased. Nearly the whole drug was released within first 15 h from the nanoparticles at pH 4.2. Since the pH of tumor tissue and endosomes is acidic, the drug is expected to be released in the targeted cancer cells. On the other hand, the release of the drug was very slow at neutral pH. The stability studies of Gemcitabine conjugated DcMNPs were carried out in neutral PBS buffer (pH 7.2). The results indicated that only 6% of Gemcitabine content was released after 6 weeks showing that DcMNPs were quite stable in PBS (pH 7.2) at 37 °C. This is a desirable property, which provides the stability of the drug in blood and also an advantage for the storage of nanoparticles.

Gemcitabine conjugated DcMNPs obtained in this study were found as nearly 6 and 3 fold more toxic on SKBR-3 and MCF-7 cells, respectively, compared to free Gemcitabine. The lower IC_{50} values of Gemcitabine conjugated DcMNPs in comparison to free Gemcitabine may be due to a more efficient intracellular uptake of DcMNPs through endocytosis.

5. Conclusion

The results of this study provide new insights to the development of targeted drug delivery systems in cancer therapy. In conclusion, Gemcitabine was effectively loaded on carboxyl-terminated half-generations of PAMAM DcMNPs. These nanoparticles have suitable size distribution, desired surface charge, high stability, and targeting properties. Besides, Gemcitabine conjugated nanoparticles were more toxic on cancer cells compared to free drug. Gemcitabine loaded DcMNPs may be a good targeted drug delivery system for clinical applications due to some advantages such as increasing the circulation life time of Gemcitabine, enhancing effective concentration at the target site, increasing the accessibility of the drug to tumor cells and preventing drug resistance.

Acknowledgments

The authors would like to thank Dr. Negar Taghavi Pourianazar, Aktan Alpsoy, Cagri Urfali, Prof. Dr. İnci Eroğlu, Dr. Rouhollah Khodadust, Assoc. Prof. Dr. Bora Mavis, and Assist. Prof. Dr. Ender Yildirim for their generous helps during this study.

References

Aggarwal, S., Gupta, S., Pabla, D., Murthy, R.S.R., 2013. Gemcitabine-loaded PLGA-PEG immunonanoparticles for targeted chemotherapy of pancreatic cancer. Cancer Nanotechnol. 4, 145–157.
Alexander, R., Greene, B., 2005. A novel phospholipid gemcitabine conjugate is able to bypass three drug-resistance mechanisms. Cancer Chemother. Pharmacol. 56, 15–21.
Arias, J.L., Gallardo, V., Gómez-Lopera, S.A., Plaza, R.C., Delgado, A.V., 2001. Synthesis and characterization of poly(ethyl-2-cyanoacrylate) nanoparticles with a magnetic core. J. Control Release 77, 309–321.
Arruebo, M., Fernández-pacheco, R., Ricardo Ibarra, M., Santamaría, Jesús, 2007. Magnetic Nanoparticles Drug Deliv. 2 (3), 22–32.
Arya, G., Vandana, M., Acharya, S., Sahoo, S.K., 2011. Enhanced antiproliferative activity of herceptin (HER2)-conjugated gemcitabine-loaded chitosan nanoparticle in pancreatic cancer therapy. Nanomedicine 7, 859–870.
Bekkara-Aounallah, F., Gref, R., Othman, M., Reddy, L.H., Pili, B., Allain, V., Bourgaux, C., Hillaireau, H., Lepetre Mouelhi, S., Desmoele, D., Nicolas, J., Chafi, N., Couvreur, P., 2008. Novel PEGylated nanoassemblies made of self-assembled squalenoyl nucleoside analogues. Adv. Funct. Mater. 18, 3715–3725.
Bildstein, L., Dubernet, C., Marsaud, V., Chacun, H., Nicolas, V., Gueutin, C., Sarasin, A., Bénech, H., Lepêtre-Mouelhi, S., Desmaële, D., Couvreur, P., 2010. Transmembrane diffusion of gemcitabine by a nanoparticulate squalenoyl prodrug: an original drug delivery pathway. J. Control Release 147, 163–170.
Bildstein, L., Dubernet, C., Couvreur, P., 2011. Prodrug-based intracellular delivery of anticancer agents. Adv. Drug Deliv. Rev. 63, 3–23.
Brusa, P., Immordino, M.L., Rocco, F., Cattel, L., 2007. Antitumor activity and pharmacokinetics of liposomes containing lipophilic gemcitabine prodrugs. Anticancer Res. 27, 195–200.
Cappella, P., Tomasoni, D., Faretta, M., Lupi, M., Montalenti, F., Viale, F., Banzato, F., D'Incalci, M., Ubezio, P., 2001. Cell cycle effects of gemcitabine. Int. J. Cancer 93, 401–408.
Cejas, M.A., Chen, C., Kinney, W.A., Maryanoff, B.E., 2007. Nanoparticles that display short collagen-related peptides: potent stimulation of human platelet aggregation by triple helical motifs. Bioconjug. Chem. 18, 1025–1027.
Chang, G., 2003. Multidrug resistance ABC transporters. FEBS Lett. 555, 102.
Chitkara, D., Mittal, A., Behrman, S.W., Kumar, N., Mahato, R.I., 2013. Self-assembling, amphiphilic polymer-gemcitabine conjugate shows enhanced antitumor efficacy against human pancreatic adenocarcinoma. Bioconjug. Chem. 24, 1161–1173.
Choi, Y.H., Yu, A.M., 2013. ABC transporters in multidrug resistance and pharmacokinetics: and strategies for drug development. Curr. Pharm. Des. 20, 793–807.
Couvreur, P., Stella, B., Harivardhan Reddy, L., Hillaireau, H., Dubernet, C., Desmaëie, D., Lepêtre-Mouelhi, S., Rocco, F., Dereuddre-Bosquet, N., Clayette, P., Rosilio, V., Marsaud, V., Renoir, J.M., Cattel, L., 2006. Squalenoyl nanomedicines as potential therapeutics. Nano Lett. 6, 2544–2548.
Dobrovolskaia, M.A., Patri, A.K., Simak, J., Hall, J.B., Semberova, J., De Paoli Lacerda, S. H., McNeil, S.E., 2012. Nanoparticle size and surface charge determine effects of PAMAM dendrimers on human platelets in vitro. Mol. Pharm. 9, 382–393.
El-Sayed, M., Ginski, M., Rhodes, C., Ghandehari, H., 2002. Transepithelial transport of poly (amidoamine) dendrimers across Caco-2 cell monolayers. J. Control Release 81, 355–365.
Ferrazzi, E., Stievano, L., 2014. Gemcitabine: monochemotherapy of breast cancer. Ann. Oncol. 17, v169–72.
Gao, F., Pan, B.F., Zheng, W.M., Ao, L.M., Gu, H.C., 2005. Study of streptavidin coated onto PAMAM dendrimer modified magnetite nanoparticles. J. Magn. Magn. Mater. 293, 48–54.
Gao, J., Gu, H., Xu, B., 2009. Multifunctional magnetic nanoparticles: design, synthesis, and biomedical applications. Acc Chem. Res. 42, 1097–1107.
Garg, T., Singh, O., Arora, S., Murthy, R.S.R., 2011. Dendrimer- a novel scaffold for drug delivery. Int. J. Pharm. Sci. Rev. Res. 7, 211–220.
Gillies, E.R., Fréchet, J.M.J., 2005. Dendrimers and dendritic polymers in drug delivery. Drug Discov. Today 10, 35–43.
Greish, K., Thiagarajan, G., Herd, H., Price, R., Bauer, H., Hubbard, D., Burckle, A., Sadekar, S., Yu, T., Anwar, A., Ray, A., Ghandehari, H., 2012. Size and surface charge significantly influence the toxicity of silica and dendritic nanoparticles. Nanotoxicology 6, 713–723.
Gupta, A.K., Gupta, M., 2005. Synthesis and surface engineering of iron oxide nanoparticles for biomedical applications. Biomaterials 26, 3995–4021.
Hodge, L.S., Taub, M.E., Tracy, T.S., 2011. Effect of its deaminated metabolite, 2,2-difluorodeoxyuridine, on the transport and toxicity of gemcitabine in HeLa cells. Biochem. Pharmacol. 81, 950–956.
Hong, S., Bielinska, A.U., Mecke, A., Keszler, B., Beals, J.L., Shi, X., Balogh, L., Orr Jr., B. G., Baker, J.R., Banaszak Holl, M.M., 2004. Interaction of poly(amidoamine) dendrimers with supported lipid bilayers and cells: hole formation and the relation to transport. Bioconjug. Chem. 15, 774–782.
Ito, A., Shinkai, M., Honda, H., Kobayashi, T., 2005. Medical application of functionalized magnetic nanoparticles. J. Biosci. Bioeng. 100, 1–11.
Jain, A., Dubey, S., Kaushik, A., Tyagi, A., 2010. Dendrimer: a complete drug carrier. Int. J. Pharm. Sci. Res. 1, 38–52.
Ji, S., Xu, J., Zhang, B., Yao, W., Xu, W., Wu, W., Xu, Y., Wang, H., Ni, Q., Hou, H., Yu, X., 2012. RGD-conjugated albumin nanoparticles as a novel delivery vehicle in pancreatic cancer therapy. Cancer Biol. Ther. 13, 206–215.
Khare, V., Singh, A., Mahajan, G., Alam, N., Kour, S., Gupta, M., Kumar, A., Singh, G., Singh, S.K., Saxena, A.K., Mondhe, D.M., 2016. Long-circulatory nanoparticles for gemcitabine delivery: Development and investigation of pharmacokinetics and in-vivo anticancer efficacy. Eur. J. Pharm. Sci. 92, 183–193.
Khodadust, R., Unsoy, G., Yalcın, S., Gunduz, G., Gunduz, U., 2013. PAMAM dendrimer-coated iron oxide nanoparticles: synthesis and characterization of different generations. J. Nanopart. Res. 15, 1488.
Kulkarni, S.A., Feng, S.S., 2013. Effects of particle size and surface modification on cellular uptake and biodistribution of polymeric nanoparticles for drug delivery. Pharm. Res. 30, 2512–2522.
Lansakara, P.D.S.P., Rodriguez, B.L., Cui, Z., 2012. Synthesis and in vitro evaluation of novel lipophilic monophosphorylated gemcitabine derivatives and their nanoparticles. Int. J. Pharm. 429, 123–134.

Liu, D., Chen, Y., Feng, X., Deng, M., Xie, G., Wang, J., Zhang, L., Liu, Q., Yuan, P., 2014. Micellar nanoparticles loaded with gemcitabine and doxorubicin showed synergistic effect. Colloids Surf. B Biointerfaces 113, 158–168.
Lunov, O., Syrovets, T., Röcker, C., Tron, K., Ulrich Nienhaus, G., Rasche, V., Mailander, V., Landfester, K., Simmet, T., 2010. Lysosomal degradation of the carboxydextran shell of coated superparamagnetic iron oxide nanoparticles and the fate of professional phagocytes. Biomaterials 31 (34), 9015–9022.
Maksimenko, A., Mougin, J., Mura, S., Sliwinski, E., Lepeltier, E., Bourgaux, C., Lepêtre, S., Zouhiri, F., Desmaële, D., Couvreur, P., 2013. Polyisoprenoyl gemcitabine conjugates self assemble as nanoparticles, useful for cancer therapy. Cancer Lett. 334, 346–353.
Martín-Banderas, L., Sáez-Fernández, E., Holgado, M.A., Durán-Lobato, M.M., Prados, J.C., Melguizo, C., Arias, J.L., 2013. Biocompatible gemcitabine-based nanomedicine engineered by Flow Focusing for efficient antitumor activity. Int. J. Pharm. 443, 103–109.
Mini, E., Nobili, S., Caciagli, B., Landini, I., Mazzei, T., 2006. Cellular pharmacology of gemcitabine. Ann. Oncol. 17, v7–12.
Mu, Q., Lin, G., Patton, V.K., Wang, K., Press, O.W., Zhang, M., 2016. Gemcitabine and chlorotoxin conjugated iron oxide nanoparticles for glioblastoma therapy. J. Mater. Chem. B 4 (1), 32–36.
Nune, S.K., Gunda, P., Thallapally, P.K., Lin, Y., Laird, M., Berkland, C.J., 2009. Nanoparticles for biomedical imaging. Expert Opin. Drug Deliv. 6, 1175–1194.
Pan, G., 2005. Studies on PEGylated and drug-loaded PAMAM dendrimers. J. Bioact. Compat. Polym. 20, 113–128.
Park, Y., Kang, E., Kwon, O.J., Park, H.K., Kim, J.H., Yun, C.O., 2010. Tumor targeted adenovirus nanocomplex ionically crosslinked by chitosan. J. Control. Release 148 (1), e124.
Parsian, M., Unsoy, G., Mutlu, P., Yalcin, S., Tezcaner, A., Gunduz, U., 2016. Loading of Gemcitabine on chitosan magnetic nanoparticles increases the anti-cancer efficacy of the drug. Eur. J. Pharm. 784, 121–128.
Pourjavadi, A., Tehrani, Z.M., 2016. Mesoporous silica nanoparticles with bilayer coating of poly (acrylic acid-co-itaconic acid) and human serum albumin (HSA): A pH-sensitive carrier for gemcitabine delivery. Mater. Sci. Eng. C 61, 782–790.
Pryor, J.B., Harper, B.J., Harper, S.L., 2014. Comparative toxicological assessment of PAMAM and thiophosphoryl dendrimers using embryonic zebrafish. Int. J. Nanomed. 9, 1947–1956.
Sun, C., Lee, J.S., Zhang, M., 2008. Magnetic nanoparticles in MR imaging and drug delivery. Adv. Drug Deliv. Rev. 60, 1252–1265.
Svenson, S., Tomalia, D.A., 2005. Dendrimers in biomedical applications–reflections on the field. Adv. Drug Deliv. Rev. 57, 2106–2129.
Svenson, S., 2009. Dendrimers as versatile platform in drug delivery applications. Eur. J. Pharm. Biopharm. 71, 445–462.
Taghavi Pourianazar, Negar, Gunduz, Ufuk, 2016. CpG oligodeoxynucleotide-loaded PAMAM dendrimer-coated magnetic nanoparticles promote apoptosis in breast cancer cells. Biomed. Pharmacother. 78, 81–91.
Taghavi Pourianazar, N., Mutlu, P., Gunduz, U., 2014. Bioapplications of poly (amidoamine) (PAMAM) dendrimers in nanomedicine. J. J. Nanopart. Res. 16, 2342.
Viota, J.L., Carazo, A., Munoz-Gamez, J., a Rudzka, K., Gómez-Sotomayor, R., Ruiz-Extremera, A., Salmerón, J., Delgado a, V., 2013. Functionalized magnetic nanoparticles as vehicles for the delivery of the antitumor drug gemcitabine to tumor cells physicochemical in vitro evaluation. Mater. Sci. Eng. C Mater. Biol. Appl. 33 (3), 1183–1192.
Wahajuddin, A.S., 2012. Superparamagnetic iron oxide nanoparticles: magnetic nanoplatforms as drug carriers. Int. J. Nanomed. 7, 3445–3471.
Yalcin, S., Erkan, M., Ünsoy, G., Parsian, M., Kleeff, J., Gündüz, U., 2014. Effect of gemcitabine and retinoic acid loaded PAMAM dendrimer-coated magnetic nanoparticles on pancreatic cancer and stellate cell lines. Biomed. Pharmacother. 68, 737–743.
Yang, Y., Sunoqrot, S., Stowell, C., Ji, J., Lee, C.W., Kim, J.W., Khan, S.A., Hong, S., 2012. Effect of size, surface charge, and hydrophobicity of poly(amidoamine) dendrimers on their skin penetration. Biomacromolecules 13, 2154–2162.
Zhang, J., Liu, D., Zhang, M., Sun, Y., Zhang, X., Guan, G., Zhao, X., Qiao, M., Chen, D., Hu, H., 2016. The cellular uptake mechanism, intracellular transportation, and exocytosis of polyamidoamine dendrimers in multidrug-resistant breast cancer cells. Int. J. Nanomedicine 11, 3677.